Near Infrared Spectrometer SIR-2 on Chandrayaan-1

Urs Mall*, Marek Banaszkiewicz, Kjell Brønstad, Susan McKenna-Lawlor, Andreas Nathues, Finn Søraas, Esa Vilenius and Kjetil Ullaland

Max-Planck-Institute for Solar System Research, 37191 Katlenburg-Lindau, Germany

Chandrayaan-1, the first Indian mission to the Moon, will provide an opportunity for *in situ* lunar observations over a two-year period from a 100 km polar orbit. A comprehensive suite of onboard instruments will include the SIR-2 near-infrared grating spectrometer. SIR-2, a pointing spectrometer, will observe the Moon in the spectral range 900–2400 nm, with a unique spectral resolution of 6 nm over a wide range of phase angles. The high resolution SIR-2 observations, particularly of the lunar far side and polar region, are expected to have a large impact on our understanding of the mineralogy and composition of the Moon.

Keywords: Chandrayaan, chemical composition, mineralogy, Moon, near-infrared, spectroscopy.

Introduction

THE peculiar way in which the Moon's surface reflects light incident from the Sun attracted the attention of early astronomers that led to frequent observations of lunar brightness. However, the first systematic attempts to measure the brightness variation over a lunation and also to record the brightness changes in selected lunar areas during a lunar day are generally attributed to W. F. Wislicenus. His measurements, completed in 1895 and published posthumously[1], are notable because of the large number of observations which were uniformly distributed over all lunar phases and included measurements at large phase angles. Once basic photometric observational facts were established, the question as to how one could restrict the number of types of materials from which the lunar surface is made became an issue. This question led in a natural way to fundamental research, which aimed at determining the factors that govern the optical scattering characteristics of complex surfaces. Early, extensive, photometric studies to achieve this goal were published by Hapke and van Horn[2]. Through this type of research, multispectral imaging of the lunar surface to infer its composition through remote sensing was enabled. Despite the enormous progress made through ground-based imaging of the Moon, it was necessary to await the data from six American and three Russian sample return missions in order to arrive at the, much awaited, lunar ground truth. While samples were systematically collected on the Moon, the question remained as to whether, sourced as they were from a relatively narrow belt at mid-latitudes, the Apollo and Luna specimens represented all major lunar geological units. Nonetheless, the accessibility of these samples made it possible to generate experimentally measured which was usable as ground truth to support remote sensing observations. The availability of laboratory spectral data cleared the way for space-based observations and investigations of the lunar mineralogical terrains on the far side of the Moon. Although Earth-based multispectral observations have been very successful with regard to observations of the lunar near side, one has had to wait for the lunar flybys of the Galileo mission in 1992 to obtain a glimpse of what lunar, multi-spectral, remote sensing information can deliver.

*For correspondence. (e-mail: mall@mps.mpg.de)

Science objective

Determinations of the chemical composition of the crust and mantle of a planet constitute the foremost important goals in planetary research. The terrestrial planets and the Moon are made up of rocks, which consist of minerals. These minerals provide a key to understanding the lunar rocks because their compositions and atomic structures reflect the physical and chemical conditions under which the rocks were formed. Thus lunar rocks provide information about the Moon's origin, the evolution of its crust, and the timing of critical local events such as volcanism and meteorite bombardment. Unfortunately, direct physical access to the Moon is presently limited to its crust, which constitutes only about 10% of its overall volume[3]. Because the Moon is not a uniform, homogeneous body, it consists of different groups of rocks formed in different ways at different times. Further, the rocks within particular groups are not necessarily identical and differ in their mineral composition, shapes and sizes, as well as in their chemical composition. The best information about the composition of the lunar crust is undoubtedly gained from returned samples. Unfortunately, these samples cannot be taken from the bedrock. The uppermost few meters of the lunar crust consists of a layer of loose, highly porous, fine, impact generated debris called the lunar soil or regolith. Beneath the regolith, which has typically a depth of 5–10 m, is either the intact rock or what has been termed the 'mega-regolith', i.e. a loose, but not very fine, layer of surface material[4]. Lunar materials have been classified on the basis of their texture and composition into four distinct groups[5]: (1) pristine highland rocks that are primordial igneous rocks uncontaminated by impact mixing; (2) pristine basaltic volcanic rocks, including lava flows and pyroclastic deposits; (3) polymict clastic breccias, impact melt rocks, and thermally metamorphosed granulitic breccias; and (4) the lunar regolith. Major rock-forming minerals on the Moon are silicates, such as feldspars (plagioclase), pyroxenes (clinopyroxenes, orthopyroxenes), olivine, and the iron–titanium-bearing mineral ilmenite. Hydrated (e.g. clays, biotite and carbonates) minerals have not been found on the Moon. This reduction in the number of possible rock-forming minerals greatly simplifies the deciphering of lunar mineralogy through remote sensing. However, one should keep in mind that certain minerals, e.g. pure feldspars, are extremely difficult to detect and can easily escape detection altogether, due to the fact that feldspars do not exhibit strong absorption features in the visible to near-infrared (NIR) spectral range. While the highly successful Clementine mission reshaped our general understanding of the Moon, exploration of the lunar crust in the NIR range has, hitherto, been rather limited. The Clementine UV-VIS camera, with its five channels in the range from 415 to 1000 nm, did allow the identification and mapping of the distribution of pyroxene-, olivine- and plagioclase-rich rocks, as well as the mapping of geographic variations in the maturity of the surface regolith at a spatial resolution comparable with ground-based telescopic studies[6–11]. However, when compared with the Clementine NIR 6 filter camera operating in the 940–2400 nm range, real spectrometers can be expected to discriminate significantly better between the different lunar mineralogies (especially with regard to the far side of the Moon, which is not accessible to high resolution spectroscopy from Earth). The SIR-2 NIR reflectance spectrometer on Chandrayaan-1, with its 256-spectral channels covering the range 0.94–2.4 micron, is intended to provide such observations. SIR-2 is designed to characterize the mineralogy of lunar surface materials in unprecedented detail and, in combination with other data sets, will enable many key questions in lunar science to be addressed (such as the temporal mineralogical evolution of mare basalts, the petrogenesis of nonmare volcanic features, etc.). The potential of this spectrometer to achieve advances will become fully apparent when its data are combined with the data from the Hyper-spectral Imager HySi (400–920 nm), also flown onboard Chandrayaan-1, providing a complete coverage from 400 to 2400 nm. SIR-2 is designed to discriminate between major minerals of the lunar surface (ortho- and clinopyroxenes, olivines, plagioclases) and to distinguish and map the petrologic types of mare and highland materials on the surface of the Moon. Further, its high spectral resolution provides the possibility to assess the content of Fe cations in pyroxenes and olivines, and to detect minor mineralogical constituents of lunar materials, e.g. spinels[12].

Returned lunar samples, ground-based spectroscopy and multicolour imaging by Clementine have revealed that lunar mare basalts are compositionally heterogeneous. This heterogeneity is thought to have resulted from magma generation processes and differentiation in the lunar interior. Compositional studies of lunar mare basalts with better spectral and spatial resolution will improve the characterization of the mafic mineralogy of the mare basalts, and especially of those located on the farside of the Moon, that occur in relatively small isolated lava ponds[13,14], and were not accessible to high resolution spectroscopy before.

Cryptomaria denote covered or hidden mare deposits that are obscured from view by emplacement of subsequent deposits of higher albedo[15]. While typical mare basalts account for ~18% coverage of the lunar surface, any major new identifications of cryptomaria would increase this fraction. This could imply that volcanism in lunar evolution was more prevalent in early lunar history than has been previously believed, suggesting a hotter lunar interior and earlier formation of melt source regions[16]. Earlier studies have documented the existence of dark-halo craters in some of these plains deposits[17], suggesting that cryptomaria can be further investigated through studies of dark halo craters. SIR-2, with its high spatial and spectral resolution, should therefore be ideally suited, through the investigation of various potential cryptomaria, to contribute to a better understanding of the extent and importance of the very earliest volcanism on the Moon.

The detection and mapping of the distribution of lunar water is an intensely debated issue, which could help to provide answers to two important questions in planetary science, i.e. to what extent is the Moon differentiated and has the volatile budget in the inner Solar System been influenced by impacting bodies? Spectroscopic VIS-NIR data should be capable of detecting water ice on the surface if the permanently shadowed areas on the lunar surface are partly illuminated by scattered radiation (so that the characteristic absorption bands of water ice are visible in the multiply-scattered light) and if the SNR of the recorded spectra taken of those areas are sufficiently high.

The SIR-2 instrument

SIR-2 is a lightweight, modular, highly compact NIR grating spectrometer based on the SIR demonstrator instrument, which was flown as part of the payload, on ESA's SMART-1 mission in 2003–2006. The SIR-2 instrument consists of three parts: the telescope, also called the Optical Box (O-Box), the Sensor-Head-Radiator-Unit (SHRU) and the Electronics (E-Box). Figure 1 shows these constituent units.

Compared to the demonstrator SIR instrument flown on SMART-1, the SIR-2 instrument has been completely upgraded. To accommodate the instrument on the Chandrayaan-1 spacecraft, the O-Box had to be physically separated from the spectrometer. In addition, the lower orbit of Chandrayaan-1 compared to SMART-1's highly elliptical orbit, led to a significant increase in the size of the radiator and required the implementation of an embedded thermoelectric cooler (TEC), and a control system to keep the detector temperature stable. Table 1 provides the mass and dimensions of the three instrument constituents.

The SIR-2 instrument collects sunlight reflected by the Moon with the help of the O-Box, which houses the optics. The housing is made of aluminum (AA 7075) and rests isostatically on three, low conducting, titanium feet ($TiAl_6V_4$), which thermally decouple this unit from the anti-sunside (ASS) extension panel on which the instrument is mounted. The outside is coated with iridite 14.2 and the inside is painted black with aeroglaze Z306. The top cover of the O-Box is painted white with PCBE. The SIR-2 front optics, which has a focal length of 180 mm, is designed to be a light collector with a low F-number (2.5). The main front mirror, whose diameter of 72 mm defines the aperture of the optics, comprises an off-axis parabolic mirror, which reflects the incoming light onto a second fold mirror. The mirrors are made of aluminum alloy (AA 6061) and coated with a gold layer. The secondary mirror reflects the light into an optical quartz fiber, which is arranged to be at the focus of the parabola such that the system's optical axis meets the centre of the fiber. The diameter of the fiber core is 400 μm, which defines the field of view (FOV) of the instrument to be 2.22 mrad = 0.127°. The fiber connecting the O-Box with the SHRU has a length of 694 mm to accommodate the O-Box and the SHRU at their designated places on the ASS-panel of the spacecraft. The physical connection between the fiber and the SHRU is achieved through a proprietary fiber design that reduces the diameter of the fiber to 250 μm inside the SHRU.

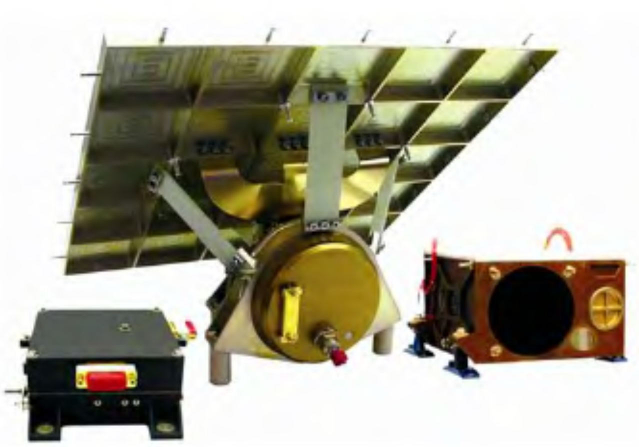

Figure 1. SIR-2 constituent units (from left to right, the E-Box, SHRU and O-Box).

Figure 2 shows schematically how the O-Box is connected to the SHRU. The SHRU consists of the spectrometer and the radiator. The spectrometer itself contains a quartz body on which a holographic corrected concave grating has been imprinted and the detector with its analogue electronics. The light enters the SHRU through the fiber, passes a blocking filter (which suppresses light between 600 and 800 nm), crosses the spectrometer slit and traverses a quartz body to reach the grating. The light dispersed by the grating then passes through the quartz body again to reach a second order filter, which is glued onto the window of the detector. The detector of SIR-2 is a linear InGaAs photodiode array (Hamamatsu InGaAs G9208-256W), which is sensitive between 0.9 and 2.55 μm. It has 256 pixels with a pixel pitch of 50 μm. The so-called Cooling Console inside the SHRU mechanically holds the detector. This structure not only supports the detector at its position but is designed to thermally decouple the detector from the sensor-head housing. By thermally decoupling the O-BOX and the SHRU from the spacecraft, the instrument can be passively cooled. The cooling console transports the heat through a heat band to the sensor-head radiator, which then radiates this energy into space. To ensure a suitable operating temperature range, a detector with an integrated thermoelectric cooler (TEC) was chosen which, together with the sensor-head radiator, forms a two-stage cooling system to maintain the temperature within the range required. Stability of the detector temperature is achieved through applying a control algorithm to the detector's thermoelectric cooler. Three voltages are required to operate the detector (Vdd = 5 V, Vref = 1.26 V and INP = 4.5 V). The power supply, together with the digital electronics of SIR-2, was built into a separate E-box which is located inside the ASS-panel of the spacecraft on which SIR-2 is located. The instrument's local harness (ILH) connects the SHRU and the E-Box. To minimize electronic noise, the E-Box was split into two compartments, with the power supply unit (PSU) in the bottom compartment and the instrument control units (ICU) in the top compartment. The ICU contains the 16-bit pixel signal ADC and the embedded

Table 1. Physical features of the SIR-2 instrument constituents

Component	Mass (g)	Envelope *x* (mm)	Envelope *y* (mm)	Envelope *z* (mm)
O-Box	611	200.0	161.0	92.7
SHRU	1444	226.9	322.9	248.6
E-Box	849	147.2	137.0	59.3

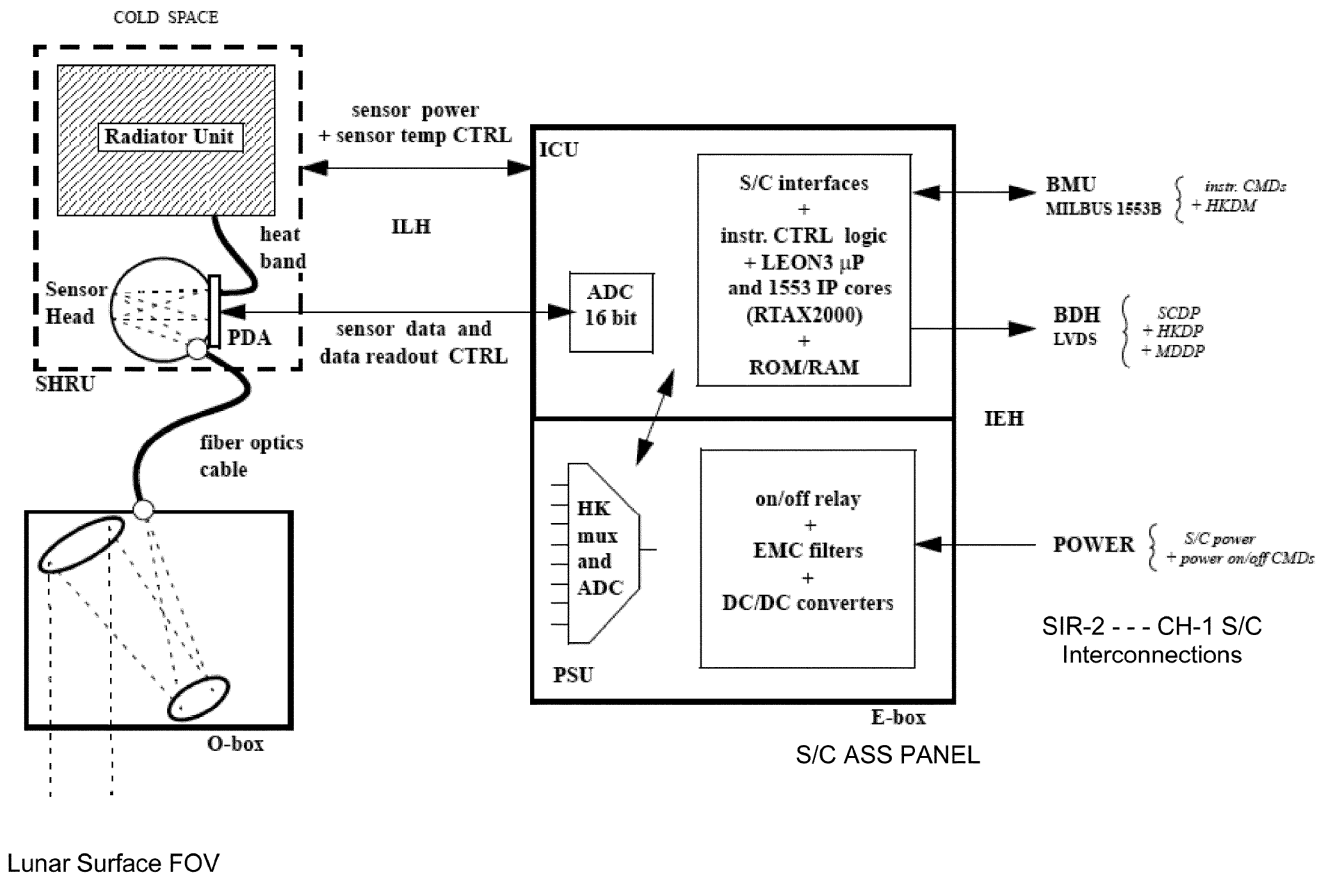

Figure 2. Schematics of the SIR-2 and its fiber design.

microprocessor and MILBUS controller for command handling, instrument control and telemetry (TM) data transfer. The PSU contains the DC/DC converter and supports the system's different voltage requirements; ON/OFF relays; the slow start and the EMC filtering (which is connected to the spacecraft's power bus). The PSU also contains the housekeeping (HK) parameter signal conditioning circuits with MUXes and the HK data ADC (16 bit) for parameter monitoring. The concept, design and the general hardware and firmware architecture of the SIR-2 ICU are described in a separate publication[18].

SIR-2 data

Transfer of information between the spacecraft and the SIR-2 instrument is handled through the spacecraft Bus Management Unit (BMU) and the Base-band Data Handling system (BDH). SIR-2 telemetry data consists of four types of data package sent via the LVDS BHD Interface: House Keeping Data Package (HKDP), SCience Data Package (SCDP), Memory Dump Data Package (MDDP) and Instrument Health Data Message (IHDM). The data packages are identified through their Application Process Identifier (APID). A subset version of the HKDP is also sent following request as IHDM over the MIL-STD-1553 BMU for real-time instrument health check. The HKDP contains the instrument housekeeping values in a 16-bit representation together with the essential instrument setup parameters and timing information. The SCDP contains the spectral data acquired from the detector. These data consist of 256 pixels, each with a resolution of 16 bits. The SCDP is transmitted as soon as its data are acquired; therefore, its transmission rate is the same as the detector sample rate. The MDDP is only sent by command, and can contain a dump of any of the memory regions of the ICU processor. This function is intended for use of diagnostics and remote instrument debugging if that should be needed. The IHDM consists of 16 (16-bit) words and is a subset of the housekeeping values in the HKDP together with additional status information. Strictly speaking it is classified as a message rather than a data packet.

Time synchronization is realized using an internal 40-bit counter to timestamp the science data. The counter, derived from the 20 MHz system clock, starts from zero after each instrument switch ON or after execution of a CPU Reset command and it increments every 10 microsec. The readings of this internal counter are synchronized with the S/C On-Boar Time (OBT) in order to enable location

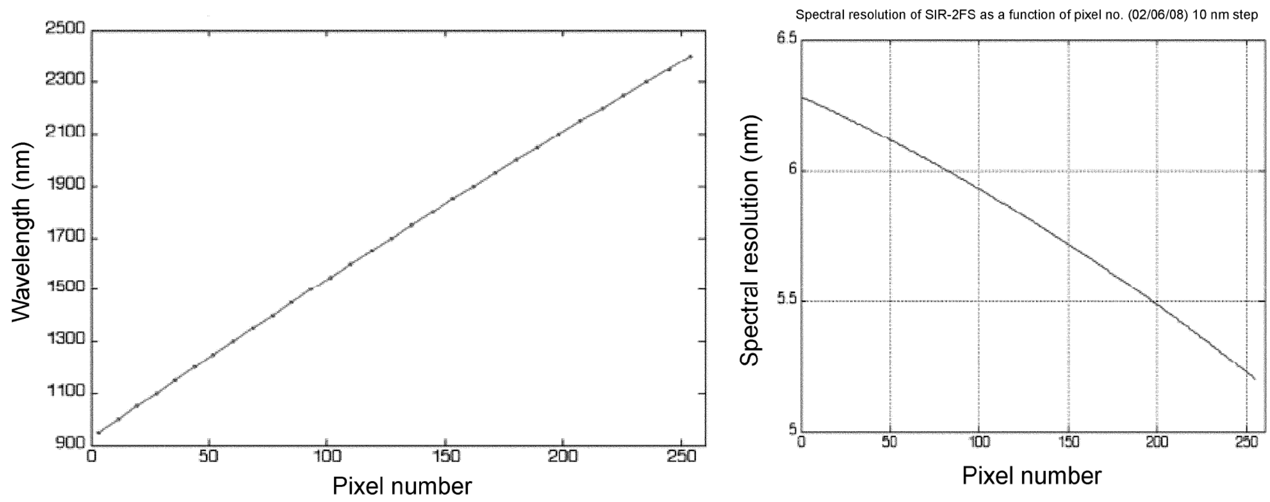

Figure 3. Measured wavelength pixel relation for SIR-2 (left plot) and the spectral resolution for SIR-2 (right plot).

Table 2. Summary of the SIR-2 instrument modes

	Mode		
Function	Standby	Preparation	Measurement
HK readout	Yes	Yes	Yes
SH powered	No	Yes	Yes
TEC control	No	Yes	Yes
HKDP transmission	Yes	Yes	Yes
SCDP transmission	No	No	Yes
MDDP transmission	Yes	Yes	Yes
IHDM transmission	Yes	Yes	Yes
Parameter upload	Yes	No	No
SH heating	Yes	No	No

of instrument FOV of the Lunar surface from the S/C aspect data. The stability of the SIR-2 counter is better than 1 microsec between synchronizations.

The SIR-2 instrument is operated in three modes, which define how the functions of the instrument are activated during its operation. They are standby- (SM), preparation- (PM), and measurement-mode (MM). These modes have to be reached in sequence. SM is the low-power idle mode entered after the instrument is switched on. PSU and ICU are ON, while the SH is OFF. TEC current is off. All instrument parameters other than the TEC current can be set from this mode. Transmission of HKDPs is enabled and transmission of IHDMs can be enabled here. The PM is used to stabilize the detector temperature before starting the measurement mode. TEC current can be set and the temperature controller can be enabled. The temperature controller will be OFF by default, and needs to be explicitly commanded ON. All parameters may be set here. HKDP transmission and IHDM transmission is possible. In MM the instrument will send SCDPs over the LVDS interface at a pre-programmed interval time. Two sub-modes are defined for the MM, namely, normal/single sampling and average/multi-sampling mode. In normal/single sampling sub-mode, each spectrum is transmitted to the ground as raw data. In average/multi-sampling mode, several preprogrammed number of spectra are averaged to improve the signal-to-noise ratio (SNR). A summary of the modes and available instrument data are given in Table 2.

Calibration

The SIR-2 instruments (FM and FS) were calibrated in October 2007 and April 2008 at ISRO's Space Applications Center (SAC) in Ahmedabad, India, and in the calibration facility at the Max-Planck Institute for Solar System Research, Germany respectively. Both spectral and radiometric calibrations were performed. The measurements included determination of the instrument's spectral range and resolution and an investigation of the pixel wavelength relation as well as measurements of the point spread function of selected pixels. One of the main goals of the calibration campaign was the determination of the instrument's performance at different temperatures at low atmospheric pressure and SIR-2 was mounted on a turntable inside the thermovac chamber for the calibration studies. All three SIR-2 constituent units were within their specified temperature ranges. Cooling was achieved by liquid nitrogen injection into the chamber's shroud. SIR-2 was co-aligned with respect to the optical axis of an illumination facility located outside the chamber. Illumination took place through an optical vacuum chamber window whose absorption characteristic is well known. For the spectral calibration, a halogen light source illuminated the entrance slit of a MS 257 monochromator available from LOT Oriel. Several data sets were taken with wavelength step sizes of 10 nm and 50 nm, covering respectively the interval 940–2410 nm and 950–2400 nm. Figure 3 shows the extracted wavelength pixel number correlation for SIR-2 and the measured spectral resolution. The measurements show clearly that the instrument has a resolution which on the average is better than 6 nm.

The pixel–wavelength relation could be fitted to the polynomial:

$$\lambda(\text{PIX})\ (\text{nm}) = 927.73 + 6.2839 \times \text{PIX} - 0.0015338 \times \text{PIX}^2 - 1.49332 \times 10^{-6} \times \text{PIX}^3.$$

This relation will be used in the data analysis chain.

1. Wirtz, C., *W. F. Wislicensus'* Selenophoto-metrische Beobachtungen. *Astron. Nachr.*, 1915, **201**, 4816–4817, 290–332.
2. Hapke, B. and van Horn, H., Photometric studies of complex surfaces, with application to the Moon. *J. Geophys. Res.*, 1962, **68**, 4545–4570.
3. Taylor, S. R., *Solar System Evolution – A New Perspective*, Cambridge University Press, 2001, 2nd edn, pp. 369–429.
4. Hartmann, W. K., Ancient lunar mega regolith and subsurface structure. *Icarus*, 1973, **18**, 634–636.
5. Stoffler, D., Knoll, H. D., Marvin, U. B., Simonds, C. H. and Warren, P. H., Recommended classification and nomenclature of lunar highland rocks. In Proceedings of Conference Lunar Highland Crust (eds Papike, J. J. and Merrill, R. B.), Pergamon Press, New York, 1980, pp. 51–70.
6. Fisher, E. M. and Pieters, C. M., Composition and exposure age of the Apollo 16 Cayley and Descartes regions from Clementine data: normalizing the optical effects of space weathering. *J. Geophys. Res.*, 1996, **100**, 2225–2234.
7. Lucey, P. G., Blewett, D. T. and Hawke, B. R., Maping the FeO and TiO_2 content of the lunar surface with multispectral imagery. *J. Geophys. Res.*, 1998, **103**, 3679–3699.
8. Pieters, C. M. and Tompkins, S., Tsiolkovsky crater: A window into crystal processes on the lunar farside. *J. Geophys. Res.*, 1999, **104**, E9, 21935–21949.
9. Staid, M. and Pieters, C. M., Integrated spectral analysis of mare soils and craters: application to eastern nearside basalts. *Icarus*, 2000, **145**, 122–145.
10. Staid, M. and Pieters, C. M., Mineralogy of the last lunar basalts. *J. Geophys. Res.*, 2001, **106**, E11, 27887–27900.
11. Gaddis, L. R., Staid, M. I., Tyburczy, J. A., Hawke, B. R. and Petro, N. E., Compositional analyses of lunar pyroclastic deposits. *Icarus*, 2003, **161**, 262–280.
12. Mao, H. K. and Bell, P. M., Crystal-field effects in spinels: oxidation states of iron and chromium. *Geochim. Cosmochim. Acta*, 1975, **39**, 865–874.
13. Yingst, R. A. and Head, J. W., Volumes of lunar lava ponds in South Pole-Aitken and Orientale Basins: implications for eruption conditions, transport mechanisms, and magma source regions. *J. Geophys. Res.*, 1997, **102**, E5, 10909–10932.
14. Yingst, R. A. and Head, J. W., Characteristics of lunar mare deposits in Smythii and Marginis basins: implications for magma transport mechanisms. *J. Geophys. Res.*, 1998, **103**, E5, 11, 135–158.
15. Head, J. W. and Wilson, L., Lunar mare volcanism: stratigraphy, eruption conditions, and the evolution of secondary crusts. *Geochim. Cosmochim. Acta*, 1992, **55**, 2155–2175.
16. Antonenko, I., Global estimates of cryptomare deposits: Implications for lunar volcanism. In 30th Annual Lunar and Planetary Science Conference, Houston, TX, 15–29 March 1999, abstract no. 1703.
17. Schultz, P. H. and Spudis, P. D., Evidence for ancient mare volcanism. In Proceedings of the Tenth Lunar Planetary Science Conference, 1979, pp. 2899–2918.
18. Torheim, O. *et al.*, Development of an embedded CPU-based Instrument Control Unit for the Chandrayaan-1 Mission to the Moon, submitted to *IEEE Trans. Geosci. Remote Sensing*, 2009.

ACKNOWLEDGEMENTS. We express our gratitude and appreciation to our colleagues Megha Bhatt, Arne Dannenberg, Prasanta Das, Edvard Fosdahl, Hermann Hartwig, Klaus Heerlein, Witold Nowosielski, Piotr Orleanski, Roman Orlik, Henry Perplies, Bjørn Pommeresche, Viviana Reimundo, Piotr Sitek, Yngve Skogseide, Arne Solberg, Olav Torheim and Mona Wedemeier without whose dedication the SIR-2 project could not have been realized. The project was funded through the Max-Planck Society, Germany and the European Space Agency. We thank the University of Bergen, Norway for support.